

Quantum Chemical Analysis of 4-Styryltriphenylamine Blue Dopant: Insights from Density Functional Theory and AIM Theory

S. Palanisamy¹, K. Selvaraju^{1*}

^{1, 1*}Department of Physics, Kandaswami Kandar's College,

Velur-638182, Namakkal (Dt), Tamilnadu, India

*Corresponding Author: physicsselvaraj[at]gmail.com

Abstract: The structural and molecular orbital analysis of 4-Styryltriphenylamine blue dopant molecule by using quantum chemical calculations have been carried out with density functional theory (DFT) and united with AIM theory. The basis sets of HF, B3LYP and B3PW91 methods were used to the geometrical parameters, bond topological analysis and electrostatic transport properties of the molecules are studied. The characterized of the molecule have been analyzed to charge density and energy density. The variation of atomic charges of the molecule has been compared to different optimized basis sets. The HOMO-LUMO gap of the molecule are calculated from different basis sets. These calculated values have been compared with the density of states spectrum (DOS). The ESP is depleted absolutely about the N-atoms and the charge accumulated of the molecule. The appreciative of the blue dopant 4-Styryltriphenylamine molecule is very useful for further a design of high efficiency, low cost and stability of OLEDs.

Keywords: OLED, AIM charge, HLG, ESP, DOS

1. Introduction

Organic Light Emitting Diodes (OLEDs) are emerging as a fore-front in organic optoelectronics research methods [1-3]. It was focused on the first observed the OLED device by use of a two layered organic thin film. Further reported a three layered device, in which a host layer is sandwiched by whole transport and electron transport layers. In addition, they reported a two layered system; in which one layer have roles of host and other layers of electron transport properties of the OLEDs materials [4, 5]. Finally, the result of these research studies in a reduction in operating voltage and improvements in efficiency. High mobility of organic electron transport materials are success of organic light emitting diode molecules. A considerable number of small molecules with electron motilities (μ e) of up to 10^{-4} e to 10^{-3} $\text{cm}^2 \text{V}^{-1} \text{s}^{-1}$ have been reported as electron transport layers (ETLs) in OLEDs [6-8]. All the possible applications of organic devices, white organic light-emitting diodes (WOLEDs) have received considerable interest due to their potential for replacing conventional lighting sources for display backlighting and solid-state lighting [9, 10]. In the particularly WOLEDs have promising properties like improved high power efficiency, high colour temperature, homogenous large area emission, low operating voltage and simple fabrication process [11-16].

Recently, the triphenylamine OLED molecule is a non-basic function. These derivatives have very useful properties in electrical conductivity and electroluminescence of the molecules. The electroluminescence of a material emits light in response to the passage of an electric current or to a strong electric field. It is used in OLEDs as hole-transporters of these derivatives [17]. Figure 1 depicts the chemical structure of 4-Styryltriphenylamine molecule is trust to be an excellent electrostatic and transport material of organic light emitting blue dopant molecule. It is used as the electron charge carrier increased to the quantum efficiency of electron [18]. The main purpose of this research article is

focus on the present theoretical investigation, the computational details, structural aspects, electron density and charge density, atomic charges, AIM charges, molecular orbital analysis and molecular electrostatic potential of the 4-Styryltriphenylamine OLED molecule have been studied.

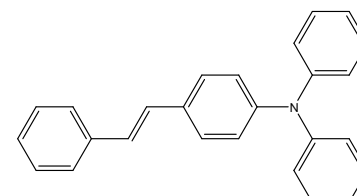


Figure 1: Chemical structure of 4-Styryltriphenylamine molecule

2. Computational Details

The 4-Styryltriphenylamine OLED molecule has been carried out with density functional theory (DFT) with the different basis sets HF, B3LYP and B3PW91 by using Gaussian09 program [19-21]. All optimized geometry (Figure 2) was performed via Berny algorithm in redundant internal co-ordinates. The threshold convergence for maximum force, root mean square (RMS) force, maximum displacement and root mean square (RMS) displacement are 0.00045, 0.0003, 0.001 and 0.0012 au respectively. The self-consistency of non-interactive wave function was performed with a requested convergence on the density matrix of 10^{-8} and 10^{-6} for the RMS and maximum density matrix error between the iterations [22]. By using Bader's theory of "Atoms in Molecules" (AIM) the bond topological and the electrostatic properties have been calculated from the EXT94b routine incorporated to the AIMPAC software [23]. To produce the deformation density and Laplacian of electron density maps are calculated from the wfn2plots and XD package [24]. The isosurface of positive and negative regions of the molecule has been plotted with Gview [25] programme. The GaussSum program has been used to

determine the density of states (DOS) of the 4-Styryltriphenylamine molecule for different optimized methods [26].

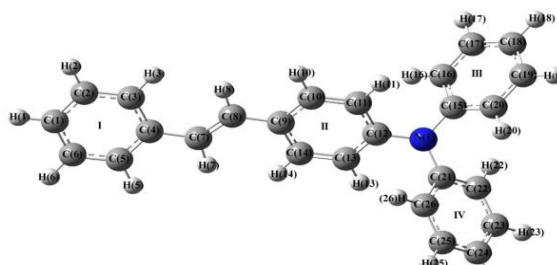


Figure 2. Optimized geometry of 4-Styryltriphenylamine molecule

3. Results and Discussion

3.1. Structural aspects

The OLED of 4-Styryltriphenylamine molecule is in excellent agreement with theoretical parameters. Recently, a several computational methods coupled with HF, B3LYP and B3PW91 have been used to analyze the geometrical parameters, electronic structure and the molecular orbitals of OLEDs molecules. The bond distance estimate the HF/6-311G **methods are found to be continues smaller than the other two methods [B3LYP/6-311G**and B3PW91/6-311G**] respectively. This 4-Styryltriphenylaminemolecule has four aromatic rings, one methyl group and the N atom is added through this optimized geometry structure. Figure 3.shows the OLED molecule has been optimized by different basis sets.

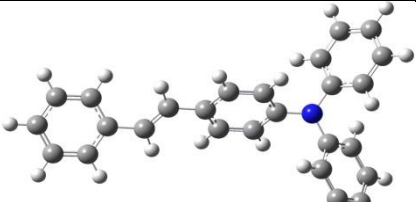
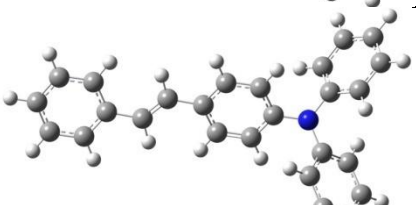
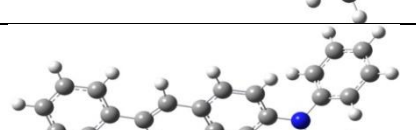
Methods	Optimized geometry
HF/ 6-311G (d, p)	
B3LYP/ 6-311G (d, p)	
B3PW91/ 6-311G (d, p)	

Figure 3: Optimized geometry of 4-Styryltriphenylamine molecule at HF, B3LYP and B3PW91 levels.

A very interesting one of the present study of these OLED molecules, the aromatic ring-I in the C–C bond lengths of the molecule are calculated from HF methods are vary from ~1.382 Å to 1.395 Å. And, these bond distance are modified from ring-II are variation from ~1.379 Å to 1.394 Å. Similarly, the aromatic rings (III and IV) of the C–C bond distances are found to be almost equal (1.383 Å to 1.390 Å). For B3LYP/6-311G** method of all C–C bonds are increases from 1.384 Å to 1.407 Å. Finally, the aromatic rings of the C–C bond distance of these optimized methods B3PW91/6-311G** are varied from (~1.382 Å to 1.405 Å). The maximum observed variation for all C–C bond is 0.028 Å (Table-1).

The ring connector of the 4-Styryltriphenylamine is varying from $\sim 1.327\text{\AA}$ to 1.478 \AA for all the optimized basis sets. The maximum observed variation is $\sim 0.151\text{ \AA}$. The N-C bond distance of the molecule is slightly modified from

(~1.414 Å to 1.417 Å) for HF methods. Notably, the N–C bonds of the molecule are increases form (~1.410 Å to 1.423 Å) compared with other two methods (B3LYP and B3PW91). However, the C–H bondlengths of the molecule range are ~1.074 Å to 1.087 Å and almost remain same for all the basis set levels. The maximum observed value is ~0.013 Å. In the attractive study of bond angles of these research studies, the bond angles of N–C–C bonds of the molecule are vary from 120.4° to 121° by calculated form HF methods. By using another two methods (B3LYP and B3PW91) these bonds are slightly modified from ~120.4° to ~121.1° respectively. Similarly, the C–N–C bonds of the molecule are calculated from ~119.9° to ~120.1° in the HF methods. However, these bonds are slightly altered from ~119.6° to ~120.4° compared with other two methods. Table-2 shows that the selected bond angles of the 4-Styryltriphenylaminemolecules are presented and compared with different optimized methods.

Table 1: Bond lengths of the 4-Styryltriphenylamine molecule at HF, B3LYP and B3PW91 levels

Bonds	HF/ 6-311G**	B3LYP/ 6-311G**	B3PW91/ 6-311G**
Ring-I			
C (1)-C (2)	1.386	1.396	1.394
C (2)-C (3)	1.382	1.388	1.386
C (3)-C (4)	1.395	1.407	1.405
C (4)-C (5)	1.392	1.406	1.403
C (5)-C (6)	1.384	1.391	1.389
C (6)-C (1)	1.383	1.392	1.390
Ring Connector			
C (4)-C (7)	1.478	1.465	1.461
C (7)-C (8)	1.327	1.346	1.346
C (8)-C (9)	1.476	1.461	1.457
Ring-II			
C (9)-C (10)	1.390	1.405	1.403
C (10)-C (11)	1.383	1.387	1.385
C (11)-C (12)	1.388	1.401	1.399
C (12)-C (13)	1.393	1.406	1.403
C (13)-C (14)	1.379	1.384	1.382
C (14)-C (9)	1.394	1.408	1.405
N-C Bonds			
N (1)-C (12)	1.414	1.416	1.410
N (1)-C (15)	1.417	1.423	1.416
N (1)-C (21)	1.417	1.422	1.416
Ring-III			
C (15)-C (16)	1.390	1.401	1.399
C (15)-C (20)	1.390	1.401	1.399
C (16)-C (17)	1.383	1.391	1.389
C (17)-C (18)	1.385	1.394	1.392
C (18)-C (19)	1.384	1.394	1.392
C (19)-C (20)	1.384	1.391	1.389
Ring-IV			
C (21)-C (26)	1.390	1.402	1.399
C (21)-C (22)	1.390	1.402	1.399
C (22)-C (23)	1.383	1.391	1.389
C (23)-C (24)	1.385	1.394	1.392
C (24)-C (25)	1.384	1.394	1.392
C (25)-C (26)	1.384	1.391	1.389
C-H Bonds			
C (1)-H (1)	1.075	1.084	1.085
C (2)-H (2)	1.076	1.085	1.085
C (3)-H (3)	1.074	1.084	1.085
C (5)-H (5)	1.076	1.085	1.086
C (6)-H (6)	1.076	1.084	1.085
C (7)-H (7)	1.077	1.087	1.088
C (8)-H (8)	1.077	1.087	1.088
C (10)-H (10)	1.076	1.085	1.086
C (11)-H (11)	1.074	1.083	1.084
C (13)-H (13)	1.074	1.083	1.084
C (14)-H (14)	1.075	1.084	1.085
C (16)-H (16)	1.074	1.083	1.084
C (17)-H (17)	1.076	1.084	1.085
C (19)-H (19)	1.076	1.084	1.085
C (20)-H (20)	1.074	1.084	1.085
C (18)-H (18)	1.075	1.083	1.084
C (22)-H (22)	1.074	1.083	1.084
C (23)-H (23)	1.076	1.084	1.085
C (24)-H (24)	1.075	1.084	1.085
C (25)-H (25)	1.076	1.084	1.085
C (26)-H (26)	1.074	1.083	1.084

Table 2: Bond angles ($^{\circ}$) the 4-Styryltriphenylamine molecule at HF, B3LYP and B3PW91 levels

Bonds	HF/6-311G**	B3LYP/6-311G**	B3PW91/6-311G**
N (1)-C (12)-C (11)	121.0	121.0	121.1
N (1)-C (12)-C (13)	120.6	120.8	120.6
N (1)-C (15)-C (16)	120.4	120.5	120.6
N (1)-C (15)-C (20)	120.6	120.5	120.4
N (1)-C (21)-C (22)	120.4	120.4	120.4
N (1)-C (21)-C (26)	120.6	120.6	120.5
C (12)-N (1)-C (15)	120.1	120.1	119.6
C (12)-N (1)-C (21)	120.0	120.4	120.0
C (15)-N (1)-C (21)	119.9	119.6	120.4

3.2 Electron Density and Charge Density

The most important role of the organic light emitting diodes of 4-Styryltriphenylamine molecule is plotted in deformation density maps as shown in Figure 4. (a)-(c). The bond critical point having the Eigen values are calculated at a point (3, -1). The bond topological parameters, electron density, Laplacian of electron density, bond ellipticity and eigen value for all the bonds have been calculated from Table-3. The HF methods represent the high electron density (ring-I) at bond critical points of the C–C bond distance of the molecule are $2.204 \text{ e}\text{\AA}^{-3}$ to $2.160 \text{ e}\text{\AA}^{-3}$. The second optimized method B3LYP of the molecule, the C–C bonds are slightly decreases from $2.106 \text{ e}\text{\AA}^{-3}$ to $2.040 \text{ e}\text{\AA}^{-3}$. The final optimized methods of the B3PW91 basis set, the C–C bond distances are decreases from $2.105 \text{ e}\text{\AA}^{-3}$ to $2.042 \text{ e}\text{\AA}^{-3}$. The maximum observed variations in the ring-I for all C–C bonds are $\sim 0.164 \text{ e}\text{\AA}^{-3}$. Similarly, the aromatic ring-II of the 4-Styryltriphenylamine molecule of C–C bonds for HF methods are slightly varied from $2.209 \text{ e}\text{\AA}^{-3}$ to $2.182 \text{ e}\text{\AA}^{-3}$. Both methods of the C–C bonds are increases from $2.115 \text{ e}\text{\AA}^{-3}$ to $2.038 \text{ e}\text{\AA}^{-3}$ for B3LYP and B3PW91 respectively. The maximum observed variation for all C–C bonds are $\sim 0.171 \text{ e}\text{\AA}^{-3}$ and compared with ring-I of the molecule. The aromatic ring connectors of the molecule are differently changed. These changes are ($\sim 1.945 \text{ e}\text{\AA}^{-3}$ to $\sim 1.886 \text{ e}\text{\AA}^{-3}$) for all optimized methods. Finally, the aromatic ring-III and ring-IV of the C–C bonds of the molecule are varied from ($\sim 2.196 \text{ e}\text{\AA}^{-3}$ to $\sim 2.069 \text{ e}\text{\AA}^{-3}$). The maximum observed variation for all C–C bonds are $\sim 0.127 \text{ e}\text{\AA}^{-3}$ respectively. The C–H bonds of high electron density at BCP of the molecule are difference from $\sim 1.988 \text{ e}\text{\AA}^{-3}$ to $\sim 1.883 \text{ e}\text{\AA}^{-3}$ for all the methods. Further, this study of 4-Styryltriphenylamine molecule; the BCP was located almost equally distant from each atom in every C–C bonds and also for N–C bonds.

In the present computational study, interesting deals with the Laplacian of the electron density give some idea about the nature of the bonds. The values of the Laplacian will show whether the bond is concentrated or depleted. The Laplacian of electron density was calculated and tabulated (Table-3). From this study, the N–C bonds of the molecule (negative value) are varying from $-18.85 \text{ e}\text{\AA}^{-5}$ to $-18.49 \text{ e}\text{\AA}^{-5}$ for all the optimized methods. Apart from these bonds, the C–C bond distances of the Laplacian of charge density are around ($-25.03 \text{ e}\text{\AA}^{-5}$ to $-16.65 \text{ e}\text{\AA}^{-5}$). Whereas, the C–H bond distance of the 4-Styryltriphenylamine molecule are increasing from $-26.59 \text{ e}\text{\AA}^{-5}$ to $-22.81 \text{ e}\text{\AA}^{-5}$ are found to be unequal. Figure 5 (a)-(c) represents the Laplacian of electron density of 4-Styryltriphenylamine molecule at HF, B3LYP and B3PW91 optimized methods.

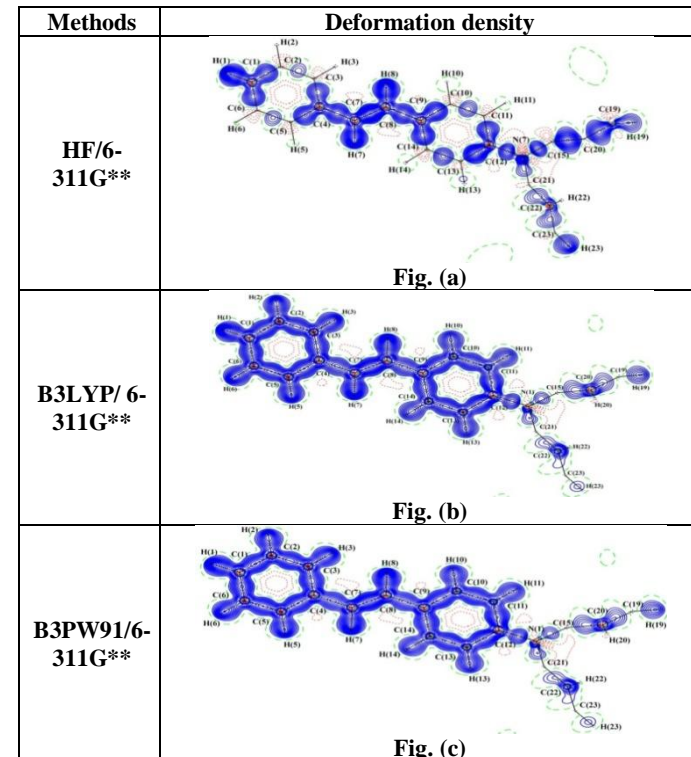
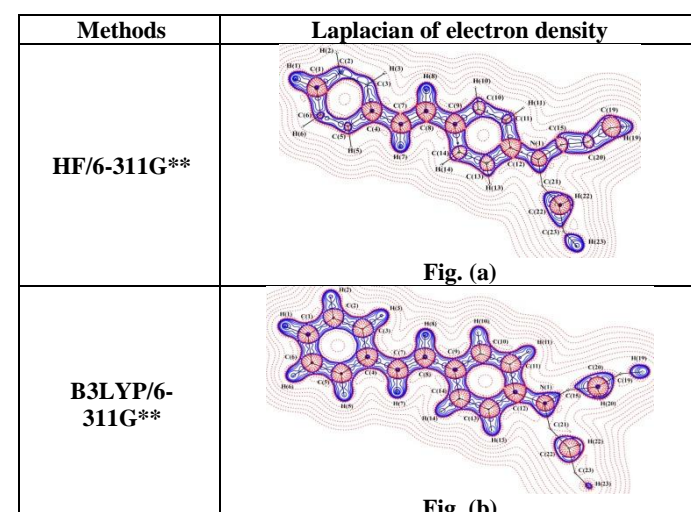


Figure 4 (a)-(c) Shows the deformation density maps of 4-Styryltriphenylamine molecule at HF, B3LYP and B3PW91 level. The positive contours (solid lines) and negative contours (dotted lines) and zero contours (dashed lines) are drawn at $\pm 0.05 \text{ e}\text{\AA}^{-3}$ intervals.



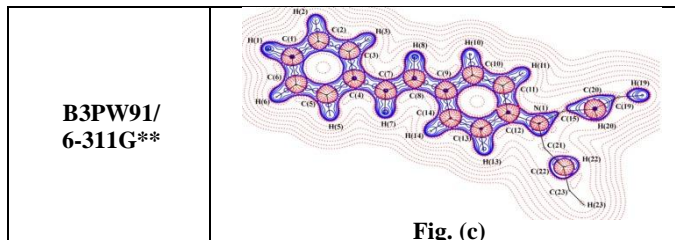


Fig. (c)

Figure 5. (a)-(c). The Laplacian of electron density of 4-Styryltriphenylamine molecule at HF, B3LYP and B3PW91 methods. The contours are drawn in logarithmic scale, $3.0 \times 2^N e^{-5}$.

The electron density distribution at the bond critical points of molecules can be calculated from the bond ellipticity (ϵ). In generally, the bond ellipticity has been defined as, measuring the anisotropy of the electron distribution at r_p . It

is measure that the density is preferentially accumulated in a given plane containing the both plane. It is expressed as, $\epsilon = (\lambda_1 / \lambda_2) - 1$. Where, λ_1 and λ_2 are the negative eigen value of Hessian matrix [27, 28]. The positive value indicates contraction of electron density. Thus, ϵ is a measure of the character of the bonding up to the limit of the double bond for which the ellipticity reaches a maximum on going from a double to a triple bond, the trend is reversed and the ellipticity decreases with increasing bond order. The mean value of C–C bonds slightly increases from 0.09 to 0.42 for all methods. The average values of N–C bonds are found to be small and around 0.06 to 0.10. Similarly, the C–H bonds of the molecule are modified around 0.023 for all the methods. The bond ellipticity (ϵ) values are calculated from Table-3.

Table 3: Bond topological properties of 4-Styryltriphenylamine molecule at HF, B3LYP and B3PW91 methods

Bonds	$\rho_{BCP(r)}$ ^a	$\nabla^2 \rho_{BCP(r)}$ ^b	ϵ^c	λ_1^d	λ_2^d	λ_3^d	d_1	d_2	D
Ring-I									
C (1)-C (2)	2.189	-24.841	0.228	-16.782	-13.667	5.608	0.691	0.695	1.386
	2.080	-20.709	0.195	-15.533	-13.000	7.824	0.697	0.699	1.396
	2.079	-20.696	0.195	-15.352	-12.843	7.500	0.696	0.698	1.394
C (2)-C (3)	2.204	-25.022	0.244	-16.934	-13.613	5.526	0.690	0.691	1.382
	2.106	-21.070	0.214	-15.781	-12.995	7.707	0.694	0.695	1.388
	2.105	-21.036	0.215	-15.589	-12.829	7.383	0.692	0.694	1.386
C (3)-C (4)	2.160	-24.157	0.227	-16.484	-13.438	5.764	0.691	0.704	1.395
	2.040	-19.894	0.186	-15.125	-12.756	7.986	0.700	0.707	1.407
	2.042	-19.946	0.187	-14.985	-12.630	7.669	0.706	0.699	1.405
C (4)-C (5)	2.177	-24.466	0.236	-16.691	-13.504	5.728	0.692	0.700	1.392
	2.053	-20.140	0.196	-15.312	-12.807	7.979	0.700	0.705	1.406
	2.054	-20.170	0.196	-15.160	-12.672	7.662	0.699	0.704	1.403
C (5)-C (6)	2.196	-24.911	0.236	-16.850	-13.635	5.574	0.691	0.693	1.384
	2.098	-20.980	0.206	-15.708	-13.026	7.754	0.695	0.696	1.391
	2.097	-20.967	0.207	-15.528	-12.868	7.429	0.693	0.695	1.389
C (6)-C (1)	2.201	-25.034	0.235	-16.903	-13.684	5.554	0.690	0.694	1.383
	2.093	-20.921	0.202	-15.663	-13.034	7.776	0.695	0.697	1.392
	2.092	-20.900	0.202	-15.477	-12.875	7.452	0.696	0.694	1.390
Ring Connector									
C (4)-C (7)	1.876	-19.510	0.088	-13.629	-12.529	6.648	0.741	0.737	1.478
	1.835	-16.646	0.105	-13.159	-11.912	8.424	0.734	0.731	1.465
	1.843	-16.813	0.105	-13.096	-11.847	8.130	0.732	0.729	1.461
C (7)-C (8)	2.400	-28.043	0.420	-19.035	-13.402	4.393	0.661	0.666	1.327
	2.258	-23.500	0.310	-17.303	-13.206	7.008	0.672	0.675	1.346
	2.252	-23.339	0.312	-17.043	-12.991	6.695	0.671	0.674	1.346
C (8)-C (9)	1.879	-19.551	0.093	-13.669	-12.507	6.626	0.739	0.737	1.476
	1.844	-16.792	0.110	-13.250	-11.937	8.395	0.730	0.731	1.461
	1.851	-16.936	0.111	-13.177	-11.859	8.100	0.728	0.729	1.457
Ring-II									
C (9)-C (10)	2.182	-24.563	0.240	-16.754	-13.508	5.699	0.698	0.692	1.390
	2.054	-20.148	0.197	-15.319	-12.799	7.969	0.701	0.704	1.405
	2.054	-20.165	0.198	-15.160	-12.657	7.653	0.700	0.703	1.403
C (10)-C (11)	2.195	-24.812	0.244	-16.821	-13.523	5.531	0.693	0.690	1.383
	2.105	-21.020	0.219	-15.761	-12.930	7.671	0.693	0.695	1.387
	2.103	-20.972	0.220	-15.563	-12.755	7.346	0.692	0.694	1.385
C (11)-C (12)	2.199	-24.982	0.271	-17.114	-13.466	5.598	0.668	0.720	1.388
	2.070	-20.400	0.227	-15.602	-12.720	7.922	0.682	0.720	1.402
	2.069	-20.405	0.226	-15.428	-12.582	7.606	0.719	0.681	1.400
C (12)-C (13)	2.182	-24.709	0.259	-16.945	-13.455	5.691	0.722	0.672	1.393
	2.054	-20.155	0.218	-15.453	-12.686	7.984	0.685	0.721	1.406
	2.056	-20.202	0.217	-15.301	-12.567	7.666	0.684	0.720	1.404
C (13)-C (14)	2.209	-25.029	0.255	-16.967	-13.520	5.457	0.690	0.689	1.379
	2.114	-21.131	0.227	-15.844	-12.909	7.621	0.690	0.694	1.384
	2.115	-21.123	0.229	-15.664	-12.749	7.289	0.689	0.693	1.382
C (14)-C (9)	2.160	-24.172	0.227	-16.494	-13.443	5.765	0.696	0.698	1.394

	2.038	-19.877	0.186	-15.116	-12.748	7.987	0.703	0.704	1.408
	2.039	-19.905	0.186	-14.964	-12.614	7.674	0.703	0.702	1.405
N-C Bonds									
N (1)-C (15)	1.933	-18.493	0.066	-13.990	-13.123	8.620	0.931	0.486	1.417
	1.886	-18.568	0.093	-13.542	-12.387	7.361	0.874	0.550	1.423
	1.905	-18.710	0.091	-13.486	-12.362	7.139	0.880	0.536	1.416
N (1)-C (12)	1.945	-18.516	0.063	-14.091	-13.256	8.831	0.485	0.929	1.414
	1.910	-18.788	0.102	-13.739	-12.468	7.419	0.543	0.873	1.416
	1.927	-18.847	0.098	-13.666	-12.451	7.270	0.531	0.879	1.409
N (1)-C (21)	1.934	-18.492	0.066	-13.998	-13.137	8.644	0.486	0.931	1.417
	1.889	-18.586	0.095	-13.566	-12.389	7.368	0.874	0.548	1.422
	1.905	-18.727	0.091	-13.489	-12.367	7.129	0.537	0.879	1.416
Ring-III									
C (15)-C (16)	2.190	-24.808	0.269	-17.033	-13.421	5.647	0.721	0.670	1.391
	2.071	-20.397	0.230	-15.628	-12.706	7.937	0.718	0.684	1.402
	2.069	-20.393	0.229	-15.442	-12.568	7.617	0.718	0.682	1.400
C (15)-C (20)	2.192	-24.829	0.270	-17.044	-13.422	5.637	0.721	0.670	1.391
	2.072	-20.414	0.230	-15.636	-12.711	7.934	0.718	0.684	1.402
	2.071	-20.421	0.229	-15.456	-12.577	7.612	0.718	0.681	1.400
C (16)-C (17)	2.194	-24.814	0.242	-16.815	-13.538	5.539	0.693	0.691	1.383
	2.092	-20.810	0.211	-15.630	-12.905	7.724	0.698	0.693	1.391
	2.091	-20.774	0.213	-15.440	-12.731	7.397	0.697	0.692	1.389
C (17)-C (18)	2.194	-24.888	0.235	-16.829	-13.630	5.571	0.699	0.686	1.385
	2.086	-20.783	0.202	-15.595	-12.977	7.789	0.700	0.694	1.394
	2.085	-20.759	0.203	-15.409	-12.814	7.464	0.699	0.693	1.392
C (18)-C (19)	2.196	-24.917	0.236	-16.848	-13.633	5.564	0.698	0.686	1.384
	2.087	-20.795	0.202	-15.603	-12.979	7.786	0.700	0.694	1.394
	2.086	-20.777	0.203	-15.420	-12.818	7.461	0.699	0.692	1.392
C (19)-C (20)	2.193	-24.785	0.241	-16.795	-13.536	5.547	0.693	0.691	1.384
	2.091	-20.797	0.211	-15.621	-12.904	7.728	0.698	0.693	1.391
	2.091	-20.780	0.212	-15.440	-12.739	7.398	0.697	0.692	1.389
Ring-IV									
C (21)-C (22)	2.190	-24.814	0.269	-17.031	-13.424	5.642	0.721	0.670	1.391
	2.070	-20.387	0.229	-15.614	-12.706	7.933	0.719	0.683	1.402
	2.071	-20.423	0.229	-15.460	-12.580	7.617	0.718	0.682	1.400
C (21)-C (26)	2.190	-24.802	0.269	-17.028	-13.413	5.639	0.669	0.721	1.391
	2.069	-20.362	0.229	-15.603	-12.693	7.934	0.683	0.719	1.402
	2.070	-20.402	0.229	-15.450	-12.570	7.618	0.682	0.718	1.400
C (22)-C (23)	2.194	-24.811	0.242	-16.813	-13.538	5.540	0.693	0.691	1.383
	2.092	-20.807	0.212	-15.630	-12.901	7.724	0.698	0.693	1.391
	2.091	-20.787	0.212	-15.444	-12.741	7.397	0.692	0.697	1.389
C (23)-C (24)	2.194	-24.895	0.235	-16.834	-13.630	5.569	0.686	0.699	1.385
	2.086	-20.785	0.202	-15.597	-12.975	7.788	0.694	0.700	1.394
	2.085	-20.759	0.203	-15.409	-12.814	7.465	0.693	0.699	1.392
C (24)-C (25)	2.195	-24.912	0.236	-16.844	-13.632	5.564	0.699	0.686	1.384
	2.086	-20.789	0.202	-15.600	-12.976	7.786	0.700	0.694	1.394
	2.086	-20.773	0.203	-15.417	-12.818	7.462	0.699	0.693	1.392
C (25)-C (26)	2.193	-24.785	0.241	-16.798	-13.533	5.545	0.691	0.693	1.384
	2.091	-20.788	0.212	-15.620	-12.893	7.725	0.698	0.693	1.391
	2.091	-20.779	0.212	-15.439	-12.739	7.399	0.692	0.697	1.389
C-H Bonds									
C (1)-H (1)	1.979	-26.412	0.020	-18.537	-18.182	10.307	0.379	0.680	1.059
	1.901	-23.312	0.019	-18.006	-17.674	12.368	0.378	0.692	1.069
	1.896	-23.207	0.018	-17.822	-17.507	12.122	0.376	0.694	1.070
C (2)-H (2)	1.980	-26.458	0.017	-18.544	-18.228	10.314	0.379	0.680	1.059
	1.901	-23.331	0.017	-17.998	-17.704	12.371	0.378	0.692	1.070
	1.896	-23.228	0.016	-17.816	-17.536	12.125	0.695	0.376	1.071
C (3)-H (3)	1.985	-26.507	0.020	-18.584	-18.212	10.290	0.679	0.379	1.058
	1.904	-23.308	0.018	-17.982	-17.657	12.332	0.691	0.379	1.069
	1.897	-23.177	0.018	-17.784	-17.476	12.083	0.693	0.377	1.070
C (5)-H (5)	1.975	-26.283	0.020	-18.429	-18.059	10.206	0.679	0.380	1.060
	1.896	-23.136	0.019	-17.884	-17.544	12.292	0.692	0.379	1.071
	1.889	-23.019	0.019	-17.696	-17.370	12.046	0.377	0.694	1.071
C (6)-H (6)	1.980	-26.458	0.017	-18.546	-18.231	10.318	0.379	0.680	1.059
	1.901	-23.326	0.017	-17.996	-17.701	12.371	0.378	0.692	1.070
	1.895	-23.223	0.016	-17.814	-17.534	12.124	0.376	0.695	1.070
C (7)-H (7)	1.973	-26.171	0.021	-18.364	-17.978	10.170	0.382	0.679	1.061

	1.891	-22.935	0.020	-17.757	-17.414	12.236	0.692	0.381	1.073
	1.883	-22.807	0.019	-17.567	-17.234	11.993	0.379	0.694	1.073
C (8)-H (8)	1.976	-26.241	0.019	-18.395	-18.051	10.205	0.680	0.381	1.061
	1.892	-22.987	0.017	-17.778	-17.473	12.265	0.381	0.692	1.073
	1.884	-22.851	0.017	-17.584	-17.288	12.021	0.695	0.379	1.074
C (10)-H (10)	1.978	-26.374	0.018	-18.483	-18.161	10.270	0.379	0.680	1.060
	1.898	-23.193	0.018	-17.924	-17.607	12.338	0.378	0.692	1.071
	1.891	-23.076	0.017	-17.737	-17.433	12.093	0.695	0.376	1.071
C (11)-H (11)	1.986	-26.518	0.022	-18.736	-18.330	10.548	0.374	0.683	1.058
	1.908	-23.417	0.021	-18.182	-17.810	12.575	0.694	0.374	1.068
	1.900	-23.283	0.020	-17.991	-17.636	12.345	0.697	0.372	1.069
C (13)-H (13)	1.987	-26.529	0.022	-18.741	-18.339	10.551	0.683	0.375	1.058
	1.909	-23.440	0.020	-18.196	-17.832	12.587	0.694	0.374	1.068
	1.901	-23.298	0.020	-17.999	-17.652	12.354	0.372	0.697	1.069
C (14)-H (14)	1.988	-26.594	0.018	-18.637	-18.315	10.357	0.680	0.378	1.058
	1.905	-23.360	0.017	-18.026	-17.724	12.390	0.378	0.692	1.069
	1.898	-23.243	0.016	-17.836	-17.549	12.142	0.376	0.694	1.070
C (16)-H (16)	1.985	-26.485	0.022	-18.712	-18.306	10.533	0.375	0.683	1.058
	1.907	-23.411	0.020	-18.177	-17.816	12.583	0.374	0.694	1.069
	1.899	-23.270	0.020	-17.983	-17.635	12.348	0.372	0.697	1.069
C (17)-H (17)	1.981	-26.500	0.016	-18.581	-18.283	10.364	0.681	0.378	1.059
	1.903	-23.366	0.017	-18.041	-17.746	12.421	0.693	0.377	1.070
	1.897	-23.258	0.016	-17.855	-17.574	12.171	0.695	0.375	1.070
C (18)-H (18)	1.977	-26.343	0.022	-18.512	-18.105	10.273	0.680	0.379	1.059
	1.901	-23.292	0.021	-18.009	-17.645	12.362	0.692	0.378	1.069
	1.895	-23.176	0.020	-17.818	-17.466	12.108	0.694	0.376	1.070
C (19)-H (19)	1.981	-26.502	0.016	-18.583	-18.284	10.365	0.681	0.378	1.059
	1.903	-23.366	0.017	-18.040	-17.745	12.419	0.693	0.377	1.070
	1.897	-23.258	0.016	-17.853	-17.574	12.169	0.695	0.375	1.070
C (20)-H (20)	1.985	-26.497	0.022	-18.722	-18.316	10.541	0.375	0.683	1.058
	1.907	-23.412	0.020	-18.177	-17.816	12.581	0.374	0.694	1.068
	1.900	-23.278	0.020	-17.988	-17.639	12.350	0.372	0.697	1.069
C (22)-H (22)	1.985	-26.490	0.022	-18.717	-18.310	10.537	0.683	0.375	1.058
	1.907	-23.407	0.021	-18.176	-17.809	12.578	0.694	0.374	1.068
	1.899	-23.273	0.020	-17.982	-17.637	12.347	0.697	0.372	1.069
C (23)-H (23)	1.981	-26.503	0.016	-18.582	-18.285	10.364	0.681	0.378	1.059
	1.903	-23.363	0.017	-18.036	-17.743	12.415	0.693	0.377	1.070
	1.897	-23.261	0.016	-17.856	-17.577	12.172	0.695	0.375	1.070
C (24)-H (24)	1.977	-26.340	0.023	-18.510	-18.101	10.271	0.379	0.679	1.059
	1.901	-23.283	0.021	-18.003	-17.635	12.355	0.692	0.378	1.069
	1.895	-23.181	0.020	-17.822	-17.472	12.112	0.376	0.694	1.070
C (25)-H (25)	1.981	-26.502	0.016	-18.582	-18.284	10.365	0.378	0.681	1.059
	1.903	-23.364	0.017	-18.038	-17.744	12.418	0.377	0.693	1.070
	1.897	-23.262	0.016	-17.858	-17.578	12.175	0.375	0.695	1.070
C (26)-H (26)	1.985	-26.490	0.022	-18.719	-18.310	10.538	0.375	0.683	1.058
	1.908	-23.411	0.021	-18.180	-17.813	12.583	0.374	0.694	1.068
	1.899	-23.273	0.020	-17.986	-17.640	12.354	0.372	0.697	1.069

^aElectron density ($e\text{\AA}^{-3}$)^bLaplacian of Electron density ($e\text{\AA}^{-5}$)^cBond ellipticity^dHessian eigen values ($e\text{\AA}^{-5}$) and d_1 , d_2 are the distances in Å between critical point and respective atoms of the bond in Å1st line indicates to HF method2nd line indicates to B3LYP method3rdline indicates to B3PW91 method

3.3 Atomic Charges

The effective atomic charges play an interesting role in the application of quantum chemical calculation. In the polarization effects and the electrostatic interactions of the atomic charges or partial atomic charges of the molecules analyse in the chemical reactions [29, 30].The electrostatic interactions accurately calculated to the atomic charges of

some different methods such as Mulliken Population Analysis (MPA), Natural Population Analysis (NPA) and Atoms in Molecules (AIM) charges have been analysed. The AIM charges of the 4-Styryltriphenylamine molecule of all C-atoms almost found to be positive value increases from 0.010 e to 0.450 e for HF methods. Similarly, another two optimized methods of all C-atoms are almost negative value. These C-atom values are increases from -0.030 e to 0.350 e respectively. Especially, the N-atoms are almost negative value. These values are varied from -1.130 e to -1.580 e for all the optimized (HF, B3LYP and B3PW91) methods. The maximum observed variation for these atoms are ~0.45 e. The differences of AIM charges distribution for all methods are presented in Table-4. The calculated values of the MPA charges of all C-atoms vary from -0.031 e to 0.2 e by using HF methods. When the applied B3LYP and B3PW91 methods the variation of C-atoms are increases from -0.060 e to 0.137 e. The maximum observed variation in all C-

atoms are 0.17 e in all methods. Similarly, the N-atoms remain almost negative value. The variations in all optimized methods are -0.678 e to -0.498 e. The maximum observed in the N-atoms are ~0.18e. The another calculated methods of the NPA atomic charges of the 4-Styryltriphenylamine molecule of all C-atoms are found to be positive and negative values; these values are increased

from -0.231 e to 0.207 e for all basis sets. The maximum observed variations in all C-atoms are around 0.24 e. The N-atoms in the all optimized basis sets method are found to be unequal (-0.468 e to -0.576 e). The maximum observed variation in N-atoms are ~0.108 e. Table-5 shows that the MPA and NPA charges for the HF, B3LYP and B3PW91 methods of the molecule.

Table 4: AIM charge of 4-Styryltriphenylamine molecule

Atoms	HF/ 6-311G**	B3LYP/6-311G**	B3PW91/ 6-311G**
C-Atoms			
C (1)	0.020	-0.020	-0.030
C (2)	0.020	-0.010	-0.020
C (3)	0.020	-0.020	-0.030
C (4)	0.000	0.010	0.000
C (5)	0.010	-0.020	-0.030
C (6)	0.020	-0.010	-0.020
C (7)	0.020	-0.010	-0.030
C (8)	0.010	-0.010	-0.020
C (9)	0.010	0.010	0.000
C (10)	0.010	-0.010	-0.020
C (11)	0.030	-0.010	-0.030
C (12)	0.450	0.340	0.350
C (13)	0.030	-0.010	-0.020
C (14)	0.020	-0.010	-0.020
N-Atom			
N (1)	-1.580	-1.130	-1.170
C-Atoms			
C (15)	0.450	0.330	0.340
C (16)	0.030	-0.020	-0.030
C (17)	0.020	-0.010	-0.020
C (18)	0.020	-0.020	-0.030
C (19)	0.020	-0.010	-0.020
C (20)	0.030	-0.010	-0.030
C (21)	0.450	0.330	0.340
C (22)	0.030	-0.020	-0.030
C (23)	0.020	-0.010	-0.020
C (24)	0.020	-0.020	-0.030
C (25)	0.020	-0.010	-0.020
C (26)	0.030	-0.020	-0.030
H-Atoms			
H (1)	-0.010	0.020	0.030
H (2)	-0.010	0.010	0.030
H (3)	-0.020	0.010	0.020
H (5)	-0.020	0.010	0.020
H (6)	-0.010	0.020	0.030
H (7)	-0.020	0.000	0.010
H (8)	-0.020	0.000	0.010
H (10)	-0.010	0.010	0.020
H (11)	0.010	0.030	0.040
H (13)	0.010	0.030	0.040
H (14)	-0.010	0.010	0.020
H (16)	0.000	0.030	0.040
H (17)	-0.010	0.020	0.030
H (18)	-0.010	0.020	0.030
H (19)	-0.010	0.020	0.030
H (20)	0.010	0.030	0.040
H (22)	0.010	0.030	0.040
H (23)	-0.010	0.020	0.030
H (24)	-0.010	0.020	0.030
H (25)	-0.010	0.020	0.030
H (26)	0.010	0.030	0.040

Table 5: MPA, NPA charge of 4-Styryltriphenylamine molecule

Atoms	MPA	NPA
-------	-----	-----

	HF	B3LYP	B3PW91	HF	B3LYP	B3PW91
C-Atoms						
C (1)	-0.105	-0.087	-0.096	-0.190	-0.201	-0.206
C (2)	-0.077	-0.093	-0.104	-0.172	-0.191	-0.196
C (3)	-0.105	-0.060	-0.062	-0.179	-0.185	-0.189
C (4)	-0.031	-0.062	-0.081	-0.053	-0.061	-0.065
C (5)	-0.105	-0.079	-0.087	-0.176	-0.183	-0.187
C (6)	-0.079	-0.092	-0.103	-0.174	-0.195	-0.200
C (7)	-0.075	-0.076	-0.086	-0.167	-0.182	-0.187
C (8)	-0.067	-0.070	-0.078	-0.152	-0.171	-0.176
C (9)	-0.050	-0.062	-0.081	-0.084	-0.081	-0.085
C (10)	-0.078	-0.077	-0.084	-0.148	-0.166	-0.170
C (11)	-0.098	-0.090	-0.100	-0.214	-0.225	-0.231
C (12)	0.200	0.137	0.136	0.207	0.172	0.169
C (13)	-0.086	-0.086	-0.095	-0.208	-0.219	-0.224
C (14)	-0.078	-0.057	-0.059	-0.151	-0.168	-0.172
N-Atom						
N (1)	-0.678	-0.498	-0.532	-0.576	-0.476	-0.468
C-Atoms						
C (15)	0.187	0.096	0.098	0.203	0.165	0.162
C (16)	-0.108	-0.077	-0.090	-0.216	-0.222	-0.229
C (17)	-0.072	-0.091	-0.101	-0.162	-0.187	-0.191
C (18)	-0.112	-0.093	-0.103	-0.209	-0.214	-0.220
C (19)	-0.072	0.107	-0.102	-0.162	0.166	-0.191
C (20)	-0.111	-0.091	-0.092	-0.217	-0.187	-0.229
C (21)	0.190	-0.079	0.091	0.204	-0.222	0.161
C (22)	-0.109	-0.082	-0.088	-0.217	-0.223	-0.228
C (23)	-0.072	-0.092	-0.101	-0.162	-0.186	-0.191
C (24)	-0.112	-0.094	-0.103	-0.209	-0.216	-0.220
C (25)	-0.072	-0.091	-0.100	-0.162	-0.186	-0.191
C (26)	-0.113	-0.084	-0.090	-0.219	-0.224	-0.229
H-Atoms						
H (1)	0.097	0.093	0.103	0.186	0.200	0.205
H (2)	0.097	0.092	0.102	0.185	0.200	0.205
H (3)	0.094	0.087	0.099	0.185	0.196	0.202
H (5)	0.088	0.083	0.094	0.184	0.197	0.202
H (6)	0.097	0.092	0.103	0.185	0.201	0.205
H (7)	0.095	0.085	0.101	0.175	0.187	0.192
H (8)	0.094	0.086	0.101	0.175	0.187	0.193
H (10)	0.089	0.084	0.095	0.185	0.199	0.205
H (11)	0.109	0.110	0.127	0.201	0.216	0.223
H (13)	0.109	0.111	0.127	0.201	0.215	0.222
H (14)	0.095	0.089	0.100	0.187	0.199	0.205
H (16)	0.108	0.110	0.127	0.200	0.215	0.222
H (17)	0.100	0.096	0.107	0.186	0.202	0.207
H (18)	0.096	0.093	0.104	0.187	0.201	0.206
H (19)	0.100	0.096	0.106	0.186	0.202	0.207
H (20)	0.109	0.109	0.127	0.200	0.215	0.221
H (22)	0.109	0.110	0.126	0.200	0.215	0.221
H (23)	0.099	0.096	0.107	0.186	0.202	0.207
H (24)	0.096	0.093	0.104	0.187	0.201	0.206
H (25)	0.100	0.096	0.107	0.186	0.202	0.207
H (26)	0.109	0.111	0.128	0.200	0.215	0.222

4. Molecular Orbital Energies

The performance of HOMO and LUMO levels of the molecules are very important for OLEDs molecules, it's associated with a high chemical reactivity. The charge carrier injection ability can be evaluated by the energy levels of HOMO and LUMO. In addition, the frontier molecular orbitals (FMOs) provide a reasonable qualitative prediction on the excitation properties. Thus, the calculated HOMO-LUMO levels are in good agreement with the different basis methods [31-33]. The Molecular Orbital energy level diagrams of 4-Styryltriphenylamine molecule for HF,

B3LYP and B3PW91 methods are represented in Figure.6. The HOMO and LUMO levels energies of 4-Styryltriphenylamine molecule are 9.23 eV to 3.47 eV respectively (Table-6). This calculated value also compared with the density of states spectrum (DOS). Figure7. (a)- (c) shows the density of states spectrum of 4-Styryltriphenylamine molecule with different optimized levels. Significantly, the hybridization of the molecular lower level broadens the DOS peaks. The molecules are almost electron conductivity of the HLG may facilitate a large conduction through the molecule [34].

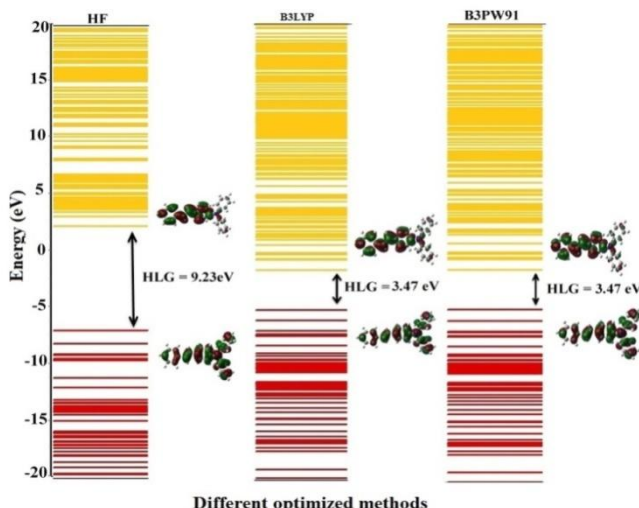


Figure 6: Shows the MO energy level diagrams of 4-Styryltriphenylamine molecule at HF, B3LYP and B3PW91 methods

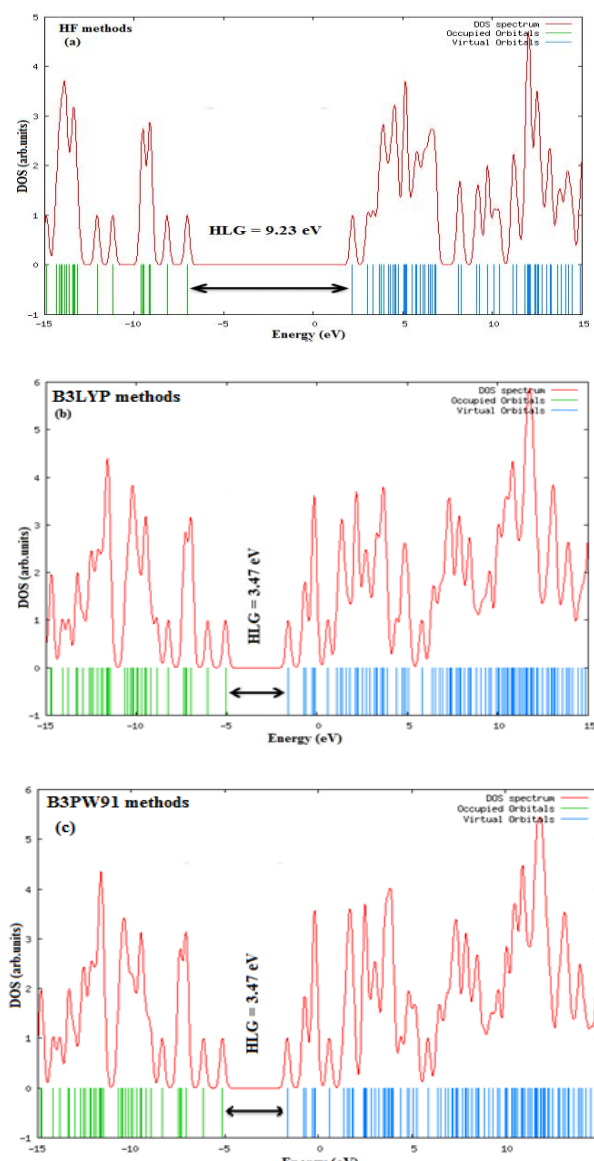


Figure 7 (a)-(c) Shows the density of states (DOS) for 4-Styryltriphenylamine molecule at HF, B3LYP and B3PW91 methods. The green line indicates HOMO and the blue line indicates LUMO levels.

Table 6: Frontier of molecular orbital energies of 4-Styryltriphenylamine molecule.

Methods	HOMO	LUMO	HLG (eV)
HF	-7.05	2.18	9.23
B3LYP	5.07	1.60	3.47
B3PW91	5.14	1.67	3.47

4.1. Electrostatic Potential

The electrostatic potential at any point in a region with electrostatic field is the work done in bringing a unit positive charge from infinity to that point (without acceleration). The electronic wave function is calculated to uniquely. Figure 8. (a)- (c) depicts the isosurface representation of Electrostatic Potential (ESP) obtained from different optimized level (HF, B3LYP and B3PW91). Both negative (red) and positive (blue) regions of this property are plotted at $\pm 0.5 \text{ e}^{-1}$ iso surface values. The negative ESP is concentrated entirely around the N-atoms, whereas in the rest of the positive ESP regions at low level [35-37]. From these studies, the H-atoms indicate the strongest attraction and the C and N atoms indicates the strongest repulsion. The electrostatic potential also calculated to the polarization of electron correlation and the charge transfer to the 4-Styryltriphenylamine OLEDs molecule.

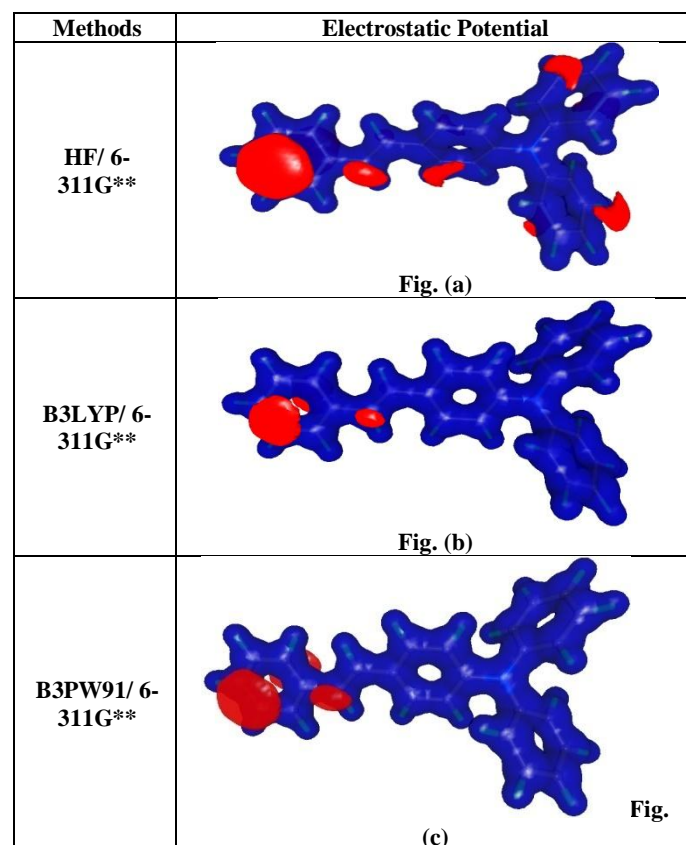


Figure 8 (a)- (c): Molecular electrostatic potential of 4-Styryltriphenylamine molecule at HF, B3LYP and B3PW91 methods. Blue: positive potential (0.05 e^{-1}), Red: negative potential (-0.05 e^{-1}).

5. Conclusion

In this investigation of research articles, the electron transport properties of 4-Styryltriphenylamine OLED

molecules are calculated from Density Functional Theory (DFT) method by using HF, B3LYP and B3PW91 basis sets to explore its structural aspects also compared. The HF methods of the molecules are analysed the geometrical parameters (Bond Length, Bond Angle) and the electrostatic transport properties of the 4-Styryltriphenylamine molecule have been premeditated and associated with other two methods. The bond topological analysis shows that the variation of charge density and Laplacian of electron density indicates the C–C bonds are much stronger than the H and N bonds in the 4-Styryltriphenylamine molecule. The HOMO-LUMO Gap of the molecule occur 9.23 eV to 3.47 eV for all optimized methods respectively. A large energy difference between the HLG frontier orbitals provides significant information regarding the softness and high reactivity of the 4-Styryltriphenylamine organic light emitting molecule. The electrostatic potential map shows that the negative potential regions are on electronegative atoms; while, the positive potential regions are around the hydrogen atoms in the molecules. These regions are change to the group charge effect. The performance of organic light emitting diode has submitted to real improvements of past years. These have been fabricated high efficiency, low cost with compared to other electron transport organic light emitting diode materials. In future this research study, these are very useful to scheme a new stability OLEDs electronics devices.

References

- [1] D. J. Gaspar and E. Polikarpov, OLED fundamentals: materials, devices, and processing of organic light-emitting diodes, CRC Press, (2015).
- [2] S.A. Van Slyke, C. Chen, C.W. Tang, Organic electroluminescent devices with improved stability, *Appl. Phys. Lett.* 1996, 69, 2160-2162.
- [3] C.W. Tang, S.A. Van Slyke, Organic electroluminescent diodes, *Appl. Phys. Lett.* 1987, 51, 913-915.
- [4] C. Adachi, S. Tokito, T. Tsutsui, S. Saito, *Jpn. J. Appl. Phys.* 1988, 27, L269.
- [5] C. Adachi, S. Tokito, T. Tsutsui, S. Saito, *Jpn. J. Appl. Phys.* 1988, 27, L713.
- [6] S. Komatsu, Y. Sakamoto, T. Suzuki, S. Tokito, *J. Solid State Chem.* 2002, 168, 470-473.
- [7] W.S. Jeon, O. Hyoung-Yun, J.S. Park, J.H. Kwon, *Mol. Cryst. Liq. Cryst.* 2011, 550, 311-319.
- [8] B. Wang, G.Y. Mu, X.L. Lv, L.X. Ma, S.Q. Zhuang, L. Wang, *Org. Electron.* 2016, 34, 179-187.
- [9] M.C. Gather, A. Köhnen, K. Meerholz, White organic light-emitting diodes, *Adv. Mater.* 2011, 23, 233-248.
- [10] B.W.D'Andrade, S.R. Forrest, White organic light-emitting devices for solid-state lighting, *Adv. Mater.*, 2004, 16, 1585-1595.
- [11] S. Reineke, M. Thomschke, B. Lüssem, K. Leo, White organic light-emitting diodes: Status and perspective, *Rev. Mod. Phys.* 2013, 85, 1245.
- [12] H. Sasabe, J. Kido, Development of high performance OLEDs for general lighting, *J. Mater. Chem. C.* 2013, 1, 1699-1707.
- [13] Z. Wu, D. Ma, Recent advances in white organic light-emitting diodes, *Mater. Sci. Eng. R-Rep.* 2016, 107, 1-42.
- [14] J. Kido, K. Hongawa, K. Okuyama, K. Nagai, White light-emitting organic electroluminescent devices using the poly (N-vinylcarbazole) emitter layer doped with three fluorescent dyes, *Appl. Phys. Lett.* 1994, 64, 815-817.
- [15] J. Kido, M. Kimura, K. Nagai, Multilayer white light-emitting organic electroluminescent device, *Science*.1995, 267, 1332.
- [16] D. Joly, D. Tondelier, V. Deborde, W. Delaunay, A. Thomas, K. Bhanuprakash, B. Geffroy, M. Hissler, R. Réau, White Organic Light-Emitting Diodes Based on Quench-Resistant Fluorescent Organ ophosphorus Dopants, *Adv. Funct. Mater.* 2012, 22, 567-576.
- [17] Wei Shi, Suqin Fan, Fei Huang, Wei Yang, Ransheng Liu and Yong Cao "Synthesis of Novel Triphenylamine-based Conjugated Polyelectrolytes and Their Application to Hole-Transport Layer in Polymeric Light-Emitting Diodes" *J. Mater. Chem.* 2006, 16, 2387-2394.
- [18] Borsenberger PM, Schein LB, Hole transport in 1-phenyl-3-((diethylamino)styryl)-5-(p-(diethylamino)phenyl) pyrazoline-doped polymers, *J PhysChem.*1994, 98:233-239.
- [19] SeminarioJ.M., PolitzerP, Molecular Density Functional theory: A tool for Chemistry, Elsevier, New York, (1995).
- [20] WadtW.R, HayP.J, *J. Chem. Phys.* 1985, 84: 82.
- [21] M.J. Frisch, G.W. Trucks, H.B. Schlegel, G.E. Scuseria, M.A. Robb, J.R. Cheeseman, J.A. Montgomery, Jr., T. Vreven, K.N. Kudin, J.C. Burant, J.M. Millam, S.S. Iyengar, J. Tomasi, V. Barone, B. Mennucci, M. Cossi, G. Scalmani, N. Rega, G.A. Petersson, H. Nakatsuji, M. Hada, M. Ehara, K. Toyota, R. Fukuda, J. Hasegawa, M. Ishida, T. Nakajima, Y. Honda, O. Kitao, H. Nakai, M. Klene, X. Li, J. E. Knox, H.P. Hratchian, J.B. Cross, C. Adamo, J. Jaramillo, R. Gomperts, R.E. Stratmann, O. Yazyev, A.J. Austin, R. Cammi, C. Pomelli, J.W. Ochterski, P.Y. Ayala, K. Morokuma, G.A. Voth, P. Salvador, J.J. Dannenberg, V.G. Zakrzewski, S. Dapprich, A.D. Daniels, M.C. Strain, O. Farkas, D.K. Malick, A.D. Rabuck, K. Raghavachari, J.B. Foresman, J.V. Ortiz, Q. Cui, A.G. Baboul, S. Clifford, J. Cioslowski, B.B. Stefanov, G. Liu, A. Liashenko, P. Piskorz, I. Komaromi, R.L. Martin, D.J. Fox, T. Keith, M.A. Al- Laham, C.Y. Peng, A. Nanayakkara, M. Challacombe, P.M.W. Gill, B. Johnson, W. Chen, M.W. Wong, C. Gonzalez, and J.A. Pople, Gaussian Inc, P. A. Pittsburgh, (2003).
- [22] B. Schlegel, *J. Comput. Chem.* 1982, 3, 214.
- [23] AIMALL (Version 10.03.25) Todd A. Keith (aim.tkgristmill.com), (2010).
- [24] Tsirelson SV, WinXPRO: A program for calculating crystal and molecular properties using multipole parameters of the electron density, *J ApplCryst.* 2002, 35:371-373.
- [25] A. Frish, E. Lecn, A.B. Nielson, A. Holder, A.J. Roy Dennington, T.A. Keith, Gaussian Incorporated, Pittsburgh PA, (2003).
- [26] Boyle N.O, GaussSum, Revision 2.1, <http://GaussSum.sf.net>.
- [27] J. M. Seminario and P. Politzer, Molecular Density Functional Theory: A Tool for Chemistry, Elesvier, New York (1995).

- [28] Srinivasan P, Asthana SN, Pawar RB, Kumaradhas P, A theoretical charge density study on nitrogen-rich 4, 4', 5, 5'-Tetranitro-2, 20-bi-1H-imidazole (TNBI) energetic molecule, StructChem, 2011, 22:1213–1220.
- [29] Mulliken, R. S. J. Chem. Phys. 1955, 23, 1833.
- [30] Jung-Goo Lee et al. An Efficient Method to Compute Partial Atomic Charges of Large Molecules Bull. Korean Chem. Soc. 2003, 24, 3.
- [31] Kan, Y.; Wang, L.; Duan, L.; Hu, Y.; Wu, G.; Qiu, Y. Appl. Phys. Lett. 2004, 84, 1513-1515.
- [32] Fleming I, Frontier orbitals and organic chemical reactions. John Wiley&sons, London, (1976).
- [33] Azizoglu A, Ozer Z, Kilic T. Collect Czech Commun, 2011, 76:95-114.
- [34] Farmanzadeh D, Ashtiani Z, Theoretical study of a conjugated aromatic molecular wire, StructChem, 2010, 21 (4):691–699.
- [35] Brinck T, Murray JS, Politzer P, The electrostatic potential: An overview, Int J QuantumChem, 1992, 44 (19):57–64.
- [36] J.S. Murray, K. Sen, Molecular Electrostatic Potential: Concepts and Applications, Theoretical and Computational Chemistry, vol. 3, Elsevier, (1996).
- [37] P. Srinivasan and A. D. Stephen, DFT and Bader's AIM analysis of 2, 5-diphenyl-1, 3, 4-oxadizole molecule: a organic light emitting diode (OLED), J. Theor. Comput. Chem. 2015, 14, (5), 1550038-1-13